

See discussions, stats, and author profiles for this publication at: <https://www.researchgate.net/publication/265172164>

# Thermophiles as Potential Source of Novel Endotoxin Antagonists: the Full Structure and Bioactivity of the Lipo-oligosaccharide from *Thermomonas hydrothermalis*

ARTICLE in CHEMBIOCHEM · AUGUST 2014

Impact Factor: 3.09 · DOI: 10.1002/cbic.201402233

---

READS

55

12 AUTHORS, INCLUDING:



[Luciana Albuquerque](#)

University of Coimbra

52 PUBLICATIONS 520 CITATIONS

SEE PROFILE



[Michelangelo Parrilli](#)

University of Naples Federico II

282 PUBLICATIONS 3,212 CITATIONS

SEE PROFILE



[Domenico Garozzo](#)

Italian National Research Council

134 PUBLICATIONS 2,612 CITATIONS

SEE PROFILE



[Maria Lina Bernardini](#)

Sapienza University of Rome

30 PUBLICATIONS 1,297 CITATIONS

SEE PROFILE

# Thermophiles as Potential Source of Novel Endotoxin Antagonists: the Full Structure and Bioactivity of the Lipo-oligosaccharide from *Thermomonas hydrothermalis*

Flaviana Di Lorenzo,<sup>[a]</sup> Ida Paciello,<sup>[b]</sup> Luigi Lembo Fazio,<sup>[b]</sup> Luciana Albuquerque,<sup>[c]</sup> Luisa Sturiale,<sup>[d]</sup> Milton S. da Costa,<sup>[c]</sup> Rosa Lanzetta,<sup>[a]</sup> Michelangelo Parrilli,<sup>[a]</sup> Domenico Garozzo,<sup>[d]</sup> Maria Lina Bernardini,<sup>[b, e]</sup> Dott. Alba Silipo,<sup>[a]</sup> and Antonio Molinaro<sup>\*[a]</sup>

*Thermomonas hydrothermalis* is a Gram-negative thermophilic bacterium that is able to live at 50 °C. This ability is attributed to chemical modifications, involving those to bacterial cell-wall components, such as proteins and (glyco)lipids. As the main component of the outer membrane of Gram-negative bacteria, lipopolysaccharides (LPSs) are exposed to the environment, thus they can undergo structural chemical changes to allow thermophilic bacteria to live at their optimal growth temperature. Furthermore, as one of the major target of the eukaryotic innate immune system, LPS elicits host immune response in a structure-dependent mode; thus the uncommon chemical

features of thermophilic bacterial LPSs might exert a different biological action on the innate immune system—an antagonistic effect, as shown in studies of LPS structure–activity relationship in the ongoing research into antagonist LPS candidates. Here, we report the complete structural and biological activity analysis of the lipo-oligosaccharide isolated from *Thermomonas hydrothermalis*, achieved by a multidisciplinary approach (chemical analysis, NMR, MALDI MS and cellular immunology). We demonstrate a tricky and interesting structure combined with a very interesting effect on human innate immunity.

## Introduction

Extremophiles are life forms capable of living in inhospitable (from a human viewpoint) environments, such as alkaline and acidic waters, boiling hot springs, high-pressure waters, ultra-saline brines, or combinations of the above chemical and physical extremes (typical for polyextremophilic microbes).<sup>[1]</sup> On the basis of optimal growth conditions, it is possible to distinguish extremophilic microorganisms as acidophiles, alcalophiles, bar-

ophiles, halophiles, psychrophiles, and thermophiles.<sup>[2]</sup> Owing to their unique features, extremophiles have attracted much interest, as they have been shown to possess high biotechnological potential in a number of important industrial applications, including bioremediation and biomining processes.<sup>[3]</sup> Among environmental factors, temperature is considered one of the most important variables for the viability and activity of microorganisms.<sup>[4]</sup> In this context, thermophiles (including Archaea, Bacteria, and Eukarya) can live and reproduce at relatively high temperatures (50–60 °C),<sup>[5]</sup> but microbes that live at temperatures above 80 °C (hyperthermophiles) have also been isolated and described.<sup>[6]</sup>

Several Gram-negative thermophilic bacteria are considered vitally important in the field of biotechnology. For instance, *Thermus aquaticus* is well known as the source of the heat-resistant enzyme Taq DNA polymerase, one of the most used enzymes in molecular biology.<sup>[5]</sup> *Thermomonas hydrothermalis* is a rod-shaped, non-motile, strictly aerobic Gram-negative bacterium with an optimum temperature for growth of about 50 °C.<sup>[7]</sup> It was isolated for the first time from hot spring at São Gemil in Central Portugal, and, on the basis of a phylogenetic analysis of the 16S rRNA gene sequence, it was considered to be closely related to another slightly thermophilic bacterium, *Thermomonas haemolytica*, although this has a lower growth temperature range than for *T. hydrothermalis*.<sup>[7]</sup> The knowledge that this microorganism has developed peculiar chemical modifications to its cell-wall components to survive at high temperatures makes *T. hydrothermalis* a fascinating bacterial


[a] Dr. F. Di Lorenzo, Prof. R. Lanzetta, Prof. M. Parrilli, D. A. Silipo, Prof. A. Molinaro  
Dipartimento di Scienze Chimiche, Università di Napoli "Federico II"  
Complesso Universitario Monte S. Angelo  
Via Cintia 4, 80126 Napoli (Italy)  
E-mail: molinaro@unina.it

[b] Dr. I. Paciello, Dr. L. L. Fazio, Prof. M. L. Bernardini  
Dipartimento di Biologia e Tecnologia "C. Darwin"  
Sapienza-Università di Roma  
Piazzale Aldo Moro 5, 00185 Roma (Italy)

[c] Dr. L. Albuquerque, Prof. M. S. da Costa  
Center for Neuroscience and Cell Biology and  
Department of Life Sciences, University of Coimbra  
3001-401 Coimbra (Portugal)

[d] Dr. L. Sturiale, Prof. D. Garozzo  
Istituto di Chimica e Tecnologia dei Polimeri-ICTP-CNR  
Via P. Gaifami 18, 95126 Catania (Italy)

[e] Prof. M. L. Bernardini  
Istituto Pasteur-Fondazione Cenci Bolognetti  
Piazzale Aldo Moro 5, 00185 Roma (Italia)  
Sapienza-Università di Roma, 00185 Roma (Italy)

 Supporting information for this article is available on the WWW under <http://dx.doi.org/10.1002/cbic.201402233>.

strain for studies to determine which alterations in the membrane constituents are associated with their extreme lifestyle.

As *T. hydrothermalis* is a Gram-negative bacterium, the outer membrane is composed essentially of lipopolysaccharides (LPSs); these amphiphilic macromolecules are involved in a variety of biological activities, they contribute to the integrity and stability of the outer membrane, and they act as a barrier against environmental stress factors, thus making them indispensable for bacterial viability in various ecosystems.<sup>[8]</sup> Moreover, in the case of microbes interacting with eukaryotes, they are recognized by the host immune system as a marker of Gram-negative bacteria and play a key role during infection: eliciting host innate and adaptive immune responses and normally resulting in elimination of the bacterium.<sup>[9]</sup> LPSs can be classified as smooth (S-LPS) or rough (R-LPS, or lipo-oligosaccharide (LOS)) on the basis of structural features; both LPS forms comprise a hydrophobic domain (lipid A) covalently linked to a non-repeating oligosaccharide region (the "core"). S-LPSs further possess a hydrophilic glycan, called the O-specific polysaccharide ("O-chain" or "O-antigen"), which is linked to the core moiety.<sup>[10,11]</sup> Lipid A, the most conserved part of the LPS molecule, commonly consists of a  $\beta$ -(1 $\rightarrow$ 6)-linked D-glucosamine disaccharide backbone substituted with a number of amide- and ester-linked fatty acids at positions 2 and 3. Furthermore, the sugar backbone is generally phosphorylated at O-1 of the GlcN I and O-4' of the GlcN II.<sup>[12]</sup> Generally, lipid A moieties are responsible for the endotoxic properties of LPS<sup>[9,13,14]</sup> as these are the portions of the macromolecules that are recognized by innate immune response receptors, such as TLR4 (toll-like receptor 4) and the MD-2 binary complex,<sup>[15]</sup> indeed, interaction of lipid A with its physiological receptors (expressed on different phagocytic cells) induces a rapid release of pro-inflammatory cytokines that, in turn, enhance the adaptive immune responses. It has been clearly demonstrated that lipid A toxicity strongly depends on its structure, in particular on the grade and distribution of the fatty acid chains, as well as on the level of phosphorylation of the diglucosamine backbone.<sup>[16,17]</sup> The core oligosaccharide moiety, composed of up to 15 sugar residues,<sup>[18,19]</sup> is characterized by the presence of a 3-deoxy-D-manno-oct-2-ulonic acid (Kdo) at first monosaccharide residue. In the case of (R)-LPSs, the core region has been shown to have antigenic properties, whereas in S forms, the antigenic determinant of the macromolecule is the O-chain,<sup>[11]</sup> usually a polysaccharide with repeating units of rarely more than five sugar residues.<sup>[20]</sup>

Because of their location, lipopolysaccharides are permanently exposed to environmental stresses that likely affect their general structure; indeed LPSs isolated from extremophilic bacteria frequently show unusual chemical characteristics that, as mentioned, influence their biological effects on the innate immune system. Interestingly, previous studies demonstrated that LPSs and LOSs of non-pathogenic bacteria can act as antagonists (or partial antagonists) towards toxic LPSs, both in vivo and in vitro.<sup>[21]</sup> In fact, because of the potentially fatal role played by LPS in sepsis, there is a continuing search for an LPS based on a natural source, that is, a LPS chemical analogue capable of binding the receptor TLR4/MD-2 complex but not

able to transmit the signal downstream (which would generate the fatal response).

Moreover, despite their key roles in the viability of Gram-negative bacteria and their potential "beneficial effects" on the innate immune system, very little is known about the structure and biological activity of lipopolysaccharides isolated from extremophilic bacteria. Thus, the structures and biological activities of lipopolysaccharide molecules isolated from *T. hydrothermalis* are fascinating to study. Here we report the complete structure of LOS extracted from *T. hydrothermalis*, the first endotoxin characterized among the genus *Thermomonas*; it possesses a unique and novel saccharide molecule. The overall structure was obtained by a combination of chemical, NMR, and MS techniques, performed on both the entire molecule and on partially or fully deacylated forms. Furthermore, a detailed study of the *T. hydrothermalis* LOS pro-inflammatory activity on human cell lines against typical virulent LPSs, such as *Escherichia coli* LPS, clearly showed its antagonist activity.

## Results and Discussion

### Extraction, purification, and compositional analysis of LOS from *T. hydrothermalis*

Crude LOS (R-LPS) was isolated from lyophilized cells of *T. hydrothermalis* strain SGM-6<sup>T</sup> by using the phenol/chloroform/light petroleum extraction protocol.<sup>[22]</sup> The presence of a rough-type LPS was confirmed by SDS-PAGE with silver nitrate staining,<sup>[23]</sup> this showed a run to the bottom of the gel due to the low molecular mass of the LOS. The material was purified from other cell contaminants by enzymatic digestion with RNase, DNase, and proteases followed by dialysis and Sephacryl HR-300 chromatography. Structural analysis<sup>[24,25]</sup> of pure LOS revealed the following monosaccharide composition: D-GalA, D-Man, D-Gal, D-GlcN (2-amino-2-deoxy-D-glucose), and 3-deoxy-D-manno-oct-2-ulonic acid (D-Kdo). Methylation analysis<sup>[26]</sup> of the intact LOS indicated the presence of 6-substituted galactofuranose, terminal galactopyranose, terminal galactopyranuronic acid, 3-substituted galactopyranose, 6-substituted aminoglucopyranose, 4,6-disubstituted mannopyranose, and 4,5-disubstituted Kdo. Analysis of the fatty acid composition, obtained by GC-MS, showed the presence of (R)-3-hydroxyundecanoic acid [11:0(3-OH)] in amide and ester linkages and undecanoic acid (11:0) exclusively in ester linkages.<sup>[25]</sup>

### Biological activity of isolated *T. hydrothermalis* LOS

In order to confirm the absence of contamination, purified LOS was analyzed for the presence of bacterial lipoproteins (BLPs) in HEK 293 cells expressing TLR2,<sup>[27]</sup> which is a pathogen recognition receptor (PRR) able to recognize, among others pathogen molecular patterns, also BLPs (Figure 1A). NF- $\kappa$ B activation was the readout in this experiment. No activation of NF- $\kappa$ B was recorded, in agreement with the chemical data, thus confirming the absence of BLP in the sample. Therefore, the biological activity of LOS was assessed in HEK293 hTLR4/CD14/MD2 cells co-transfected with a NF- $\kappa$ B-dependent luciferase.

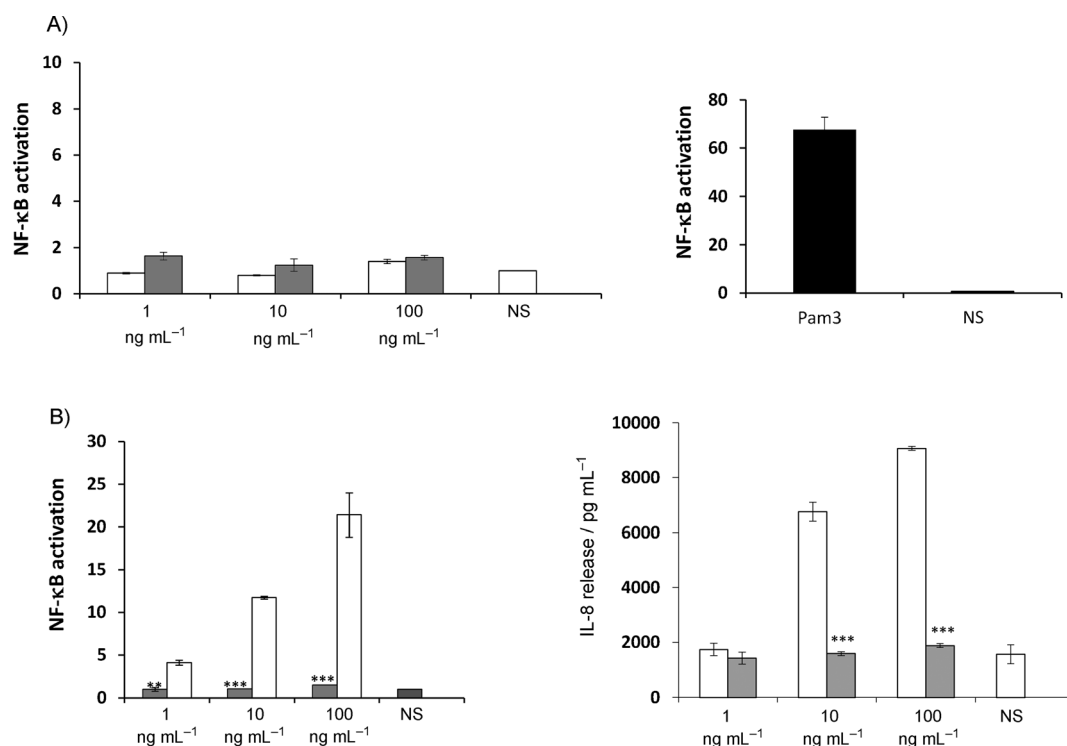


**Figure 1.** A) Assessment of contaminations in LOS. Fold of NF-κB activation upon stimulation of HEK 293 hTLR2 with 1, 10, and 100 ng mL<sup>-1</sup> of *T. hydrothermalis* LOS for 6 h. Hexa-acylated *E. coli* LPS and Pam3CSK4 were used as controls. \* $p < 0.05$ , \*\* $p < 0.01$ , \*\*\* $p < 0.001$  in the Student's t-test. *T. hydrothermalis* LOS (■) vs. *E. coli* LPS (□). B) Stimulation of HEK 293-hTLR4/MD-2/CD14 with LOS derived from *T. hydrothermalis*. Fold of activation of NF-κB and IL-8 release after 4 h of stimulation with 1, 10, and 100 ng mL<sup>-1</sup> of LOS; commercial *E. coli* LPS was used as a control. Significant difference between *T. hydrothermalis* LOS generated values and the corresponding *E. coli* LPS values are indicated (\* $p < 0.05$ ; \*\* $p < 0.01$ ; \*\*\* $p < 0.001$ ). NS: not stimulated.

Cells were exposed to different LOS concentrations (1, 10, and 100 ng mL<sup>-1</sup>). *E. coli* LPS, which has a fully hexa-acylated lipid A structure and acts as a potent agonist for TLR4/MD-2/CD14 receptors, was used as a positive control at the same concentrations. NF-κB activation was evaluated by quantifying luciferase activity after 4 h stimulation. Likewise, IL-8 release was recorded by an enzyme-linked immunosorbent assay (ELISA) after 4 h stimulation. The results show that the *T. hydrothermalis* LOS induced a significantly lower NF-κB activation than for *E. coli* LPS ( $p < 0.01$  at 1 ng mL<sup>-1</sup>,  $p < 0.001$  at 10 and 100 ng mL<sup>-1</sup>; Figure 1B). In accordance with NF-κB activation, the level of IL-8 expression was lower after stimulation with *T. hydrothermalis* LOS than for LPS from *E. coli* LPS ( $p < 0.001$  at 10 and 100 ng mL<sup>-1</sup>; Figure 1B).

We then assessed whether *T. hydrothermalis* LOS could interfere with the TLR4-mediated signaling induced by hexa-acylated lipid A. HEK 293 hTLR4 cells were pre-incubated for 1 h with different amounts (1, 10, and 100 ng mL<sup>-1</sup>) of LOS and then exposed to 10 ng mL<sup>-1</sup> hexa-acyl *E. coli* LPS for 4 h. *T. hydrothermalis* LOS significantly antagonized hexa-acyl LPS-dependent TLR4-mediated NF-κB activation and IL-8 release at 1 ng mL<sup>-1</sup> (LOS *T. hydrothermalis* vs. LPS *E. coli*:  $p < 0.05$ ; Figure 2A).

We next assessed the ability of *T. hydrothermalis* LOS to activate bone-marrow-derived macrophages (BMDMs) for cytokine production (tumor necrosis factor-α (TNF-α), keratinocyte-

derived chemokine (KC)). BMDMs were treated with 1, 10, and 100 ng mL<sup>-1</sup> *T. hydrothermalis* LOS as above, and cytokine release was recorded after 18 h (Figure 2B). Hexa-acylated *E. coli* LPS was used as a control. At all concentrations, *T. hydrothermalis* LOS elicited significantly lower amounts of TNF-α release (LOS *T. hydrothermalis* vs. LPS *E. coli*:  $p < 0.05$  at 1 and 10 ng mL<sup>-1</sup>,  $p < 0.01$  for 100 ng mL<sup>-1</sup>) and significantly lower amounts of KC release than *E. coli* LPS (LOS *T. hydrothermalis* vs. LPS *E. coli*:  $p < 0.05$  at 1 and 100 ng mL<sup>-1</sup>,  $p < 0.01$  for 10 ng mL<sup>-1</sup>; Figure 2B).

From all of these studies, it was concluded that *T. hydrothermalis* LOS is a very weak elicitor of the main cellular lines able to detect bacterial LPSs. Furthermore, it exerts an antagonist activity thus reducing hexa-acyl LPS-dependent TLR4-mediated NF-κB activation and IL-8 release (at 1 ng mL<sup>-1</sup>).

### Isolation and structural characterization of core oligosaccharide by NMR spectroscopy

The complete structure of the core oligosaccharide moiety was achieved by NMR spectroscopy and MALDI MS performed on both O-deacylated LOS and the fully deacylated form. This was essential to obtain clear information on the structure of *T. hydrothermalis* LOS. O-Deacylation was achieved by using anhydrous hydrazine.<sup>[28]</sup> The <sup>1</sup>H NMR spectrum of the O-deacylated product (Figure 3) showed anomeric signals (A–L) between

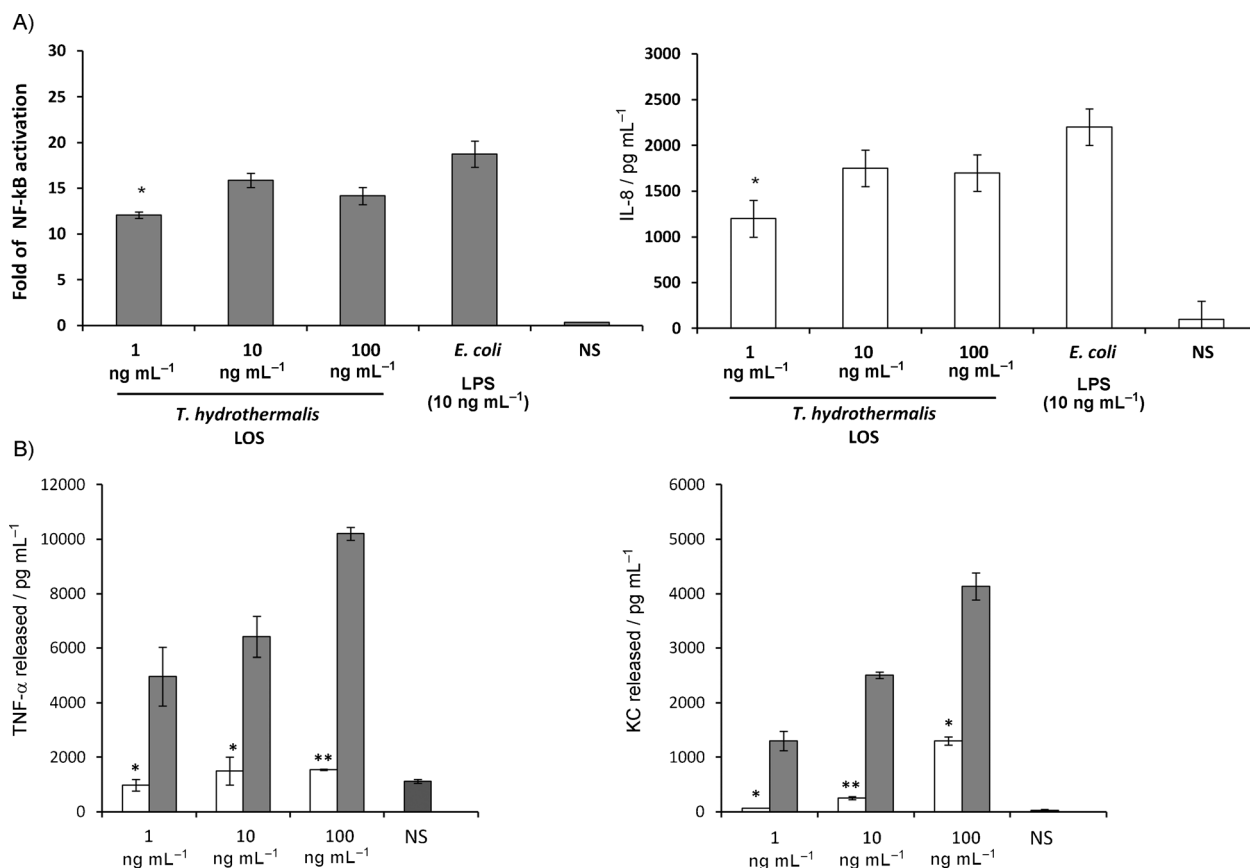


**Figure 2.** A) Competition assay. Fold of NF-κB activation and IL-8 release in HEK 293 hTLR4/MD-2/CD14 stimulated with different concentrations (1, 10, and 100 ng mL<sup>-1</sup>) of *T. hydrothermalis* LOS for 1 h and then with 10 ng mL<sup>-1</sup> *E. coli* LPS (LPS-EB ultrapure, InvivoGen) for 4 h. Significant difference between *T. hydrothermalis* LOS generated values and the corresponding *E. coli* LPS values are indicated (\* $p < 0.05$ ; \*\* $p < 0.01$ ; \*\*\* $p < 0.001$ ). B) Cytokine release in BMDMs stimulated with *T. hydrothermalis* LOS. TNF-α and KC released by BMDMs after stimulation with 1, 10, and 100 ng mL<sup>-1</sup> *T. hydrothermalis* LOS (■) and *E. coli* LPS (□) measured by ELISA at 18 h. Significant difference between *T. hydrothermalis* LOS and *E. coli* LPS are indicated (\* $p < 0.05$ ; \*\* $p < 0.01$ ; \*\*\* $p < 0.001$ ).

5.80 and 4.40 ppm (Table 1) relative to ten distinct spin systems. Complete assignment of all spin systems was achieved by tracing the spin connectivity gained from DQF-COSY and TOCSY; the correct identification of each carbon atom was achieved from the HSQC spectrum (Figure S1). Identification of the anomeric configuration of each monosaccharide residue was obtained by the intra-residual NOE contacts observed in the NOESY spectrum and the  $^3J_{\text{H1,H2}}$  coupling constants (DQF-COSY spectrum); vicinal  $^3J_{\text{H,H}}$  coupling constants allowed the assignment of the relative configuration of each monosaccharide unit. A combination of 2D homo- and heteronuclear NMR spectroscopic experiments, such as ROESY, NOESY, and HMBC, allowed the characterization of the complete oligosaccharide structure.

All residues, except residue **D**, were present as pyranose rings, as proven by the  $^{13}\text{C}$  chemical shift values, whereas the observation of correlations between protons of residue **D** and downfield-shifted carbon signals (~83.0 ppm) suggested a furanose ring, as confirmed by the intra-residual 1–4 correlations in the  $^1\text{H}$ ,  $^{13}\text{C}$  HMBC spectrum.

Residues **C** (H-1/C-1 signals at 5.54/94.3 ppm, Table 1) and **G** (H-1/C-1 signals at 4.63/101.3 ppm) were assigned to GlcpN1P and GlcpN4P of lipid A on the basis of their H-2 protons, which

showed correlations with two nitrogen-bearing carbon atoms at 53.7 and 55.3 ppm, respectively. Moreover, the multiplicity

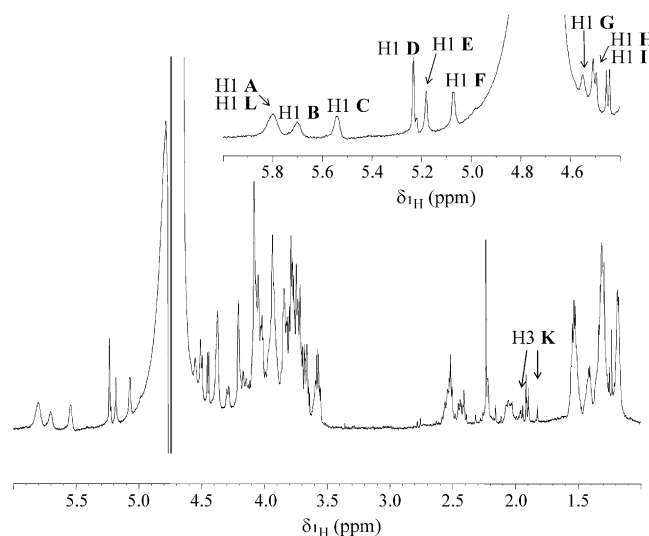


**Figure 3.**  $^1\text{H}$  NMR spectrum of O-deacylated product (anomeric region shown top right). Anomeric signals of spin systems are as in Table 1. The spectrum was recorded in  $\text{D}_2\text{O}$  at 300 K.

**Table 1.**  $^1\text{H}$ ,  $^{13}\text{C}$ , and  $^{31}\text{P}$  NMR chemical shifts of the oligosaccharide derived from O-deacylation of the LOS from *T. hydrothermalis*.

Unit	1	2	3	4	5	6	7	8
A	5.79	3.92	3.99	4.37	4.54			
<i>t</i> - $\alpha$ -GalpA1P	95.4	67.5	69.1	70.3	73.3	175.8		
	−1.73							
B	5.70	3.90	4.01	4.29	4.51	176.2		
<i>t</i> - $\alpha$ -GalpA1P	95.0	67.5	69.2	70.3	73.2			
	−2.08							
C	5.54	3.97	3.72	3.57	4.01	4.16/3.82		
6- $\alpha$ -GlcN1P	94.3	53.7	70.2	69.5	71.5	68.2		
	−1.73							
D	5.23	4.21	4.08	4.07	3.73	4.06/3.77		
6- $\beta$ -Galf	109.2	81.5	76.7	83.0	73.4	71.0		
E	5.18	4.20	3.84	4.13	3.80	4.18/3.90		
6- $\alpha$ -Manp4P	100.7	69.6	72.1	75.9	73.5	66.7		
				−1.73				
F	5.07	3.84	3.93	4.04	3.76	3.81/3.65		
<i>t</i> - $\alpha$ -Galp	99.6	69.2	69.0	69.0	70.3	62.5		
G	4.63	3.86	3.78	3.95	3.71	3.76/3.59		
6- $\beta$ -GlcN4P	101.3	55.3	72.1	76.5	75.2	63.5		
				−2.08				
H	4.50	3.68	3.72	4.08	3.73	3.64		
3- $\beta$ -Galp	102.9	70.2	80.0	68.7	75.1	61.2		
I	4.44	3.56	3.66	3.92	3.56	3.78/3.71		
<i>t</i> - $\beta$ -Galp	103.8	70.9	72.8	70.1	75.2	60.9		
K	–	–	1.97/1.72	4.02	4.17	3.67	3.98	3.81
4,5- $\alpha$ -Kdop	–	n.d.	34.8	70.0	73.0	73.1	68.0	63.2
L	5.79	3.68	3.86	4.20	4.42	–		
<i>t</i> - $\alpha$ -GalpA1P	93.4	68.4	69.4	70.5	72.3	175.8		
	−1.73							

The chemical shifts of the amide acyl chains are for 44.0; 2.17 (C2/H2); 68.5; 3.81(C3/H3); 28.9; 1.25 (CH<sub>2</sub>)<sub>n</sub>; 13.6; 0.86 (CH<sub>3</sub>). n.d.: not determined.

of the anomeric proton signal ( $^3J_{\text{H-1,P}} = 8.0$  Hz) of residue **C** and the downfield shifts of H-4 and C-4 (3.95 and 76.5 ppm, respectively) of residue **G** were diagnostic for a phosphate group linked at positions O-1 **C** and O-4 **G** (Figure 4A).<sup>[29]</sup> Inter-residue connectivity between H-1 of **G** and H-6<sub>a,b</sub> of **C**, identified in the NOESY spectrum, corroborated the assignment of residues **C** and **G** to the lipid A backbone. Spin systems **A** (H-1/C-1 at 5.79/95.4 ppm, Table 1), **B** (H-1/C-1 at 5.70/95.0 ppm) and **L** (H-1/C-1 at 5.79/93.4 ppm) were identified as  $\alpha$ -GalA residues, because of the correlation of their H-5 signals with carboxyl groups (175.8 and 176.2 ppm, respectively), thus allowing us to identify these spin systems as uronic acid residues. Their  $\alpha$ -anomeric configuration was attributed on the basis of the intra-residue NOE contact of H-1 with H-2 and the  $^1J_{\text{C1,H1}}$  and  $^3J_{\text{H1,H2}}$  values (for all three residues,  $\sim 172$  and 3.4 Hz, respectively) whereas the  $^3J_{\text{H3,H4}}$  and  $^3J_{\text{H4,H5}}$  values (3 and 1 Hz, respectively) were diagnostic of a galactose configuration. Furthermore, spin systems **A**, **B**, and **L** (**C** residue), showed the typical chemical shift and multiplicity of a phosphorylated  $\alpha$ -anomeric proton signal ( $^3J_{\text{H-1,H-2}} = 3.2$  Hz,  $^3J_{\text{H-1,P}} = 7.6$  Hz); all three residues were identified as terminal galacturonic acid residues as none of their carbon atoms was shifted by glycosylation. Residue **E** (H-1/C-1 at 5.18/100.7 ppm, Table 1) was identified as a  $\alpha$ -mannose, as shown by low  $^3J_{\text{H1,H2}}$  and  $^3J_{\text{H2,H3}}$  values (3 Hz) and by the C-3 and C-5 chemical shift values ( $\sim 72.0$  and 73.0 ppm respectively); its H-4 chemical shift was evidently displaced

downfield owing to phosphorylation (see below), whereas its C-6 was shifted downfield by glycosylation. Likewise, Kdo (residue **K**) was fully recognized and assigned by NMR starting from the diastereotopic methylene signal; it was substituted at positions O-4 and O-5 as shown by the respective carbon chemical shifts in the HSQC spectrum.

Spin systems **D**, **F**, **H**, and **I** were attributed to galactose residues. Residue **D** (H-1/C-1 at 5.23/109.2 ppm, Table 1), as described above, was shown to be a  $\beta$ -galactofuranose ( $\beta$ -Gal<sub>f</sub>) because of the typical  $^{13}\text{C}$  chemical shift of the anomeric carbon signal and the intra-residue NOE connectivity, and substituted at position O-6 because of the downfield shift of its C-6 (71.0 ppm). Likewise, **F** (H-1/C-1 at 5.07/99.6 ppm) was identified as a terminal galactose residue with an  $\alpha$ -anomeric configuration. Eventually, both **H** and **I** residues were attributed to  $\beta$ -galacto-configured sugar residues, as proven by the chemical

shift values of ring protons and the  $^3J_{\text{H,H}}$  ring coupling constants; moreover, the large  $^3J_{\text{H-1,H-2}}$  values and the NOE contacts of H-1 with H-3 and H-5 were diagnostic of the  $\beta$ -anomeric configuration. Residue **H** was substituted at position O-3, and **I** was identified as a terminal residue. The inter-residue NOE effects H-1 **H**/H-5 **K**, H-1 **E**/H-4**K**, H-1 **F**/H-6 **E**, H-1 **D**/H-3 **H**, H-1 **I**/H-6 **D** (Scheme 1) were identified in the NOESY and ROESY spectra and were confirmed by inter-residue long range scalar correlations in the HMBC spectrum (not shown).

The  $^{31}\text{P}$  NMR spectrum of the O-deacylated product revealed the presence of three phosphate signals: two overlapped, at  $-2.08$ , and  $-1.73$  ppm ( $2\times$ ). A  $^{31}\text{P}$ ,  $^1\text{H}$  HSQC experiment was performed to identify and assign the phosphate groups (Figure 4A). The  $^{31}\text{P}$  signal at  $-1.73$  showed a double set of correlations, as it consisted of two different  $^{31}\text{P}$  resonances; the anomeric proton signal of residue **A** was correlated with the  $\alpha$ -GalA **C** anomeric signal, thus showing clearly a trehalose-like linkage with a phosphodiester bond. The  $\alpha$ -GalA **L** anomeric proton signal was correlated with proton H-4 of mannose residue **E**, thus demonstrating that residue **L** is linked to **E** by a phosphodiester bond. Likewise, the phosphorous signal at  $-2.08$  ppm was shown to be related to a double correlation with two different proton signals, at 5.70 ppm (H-1 **B**) and 3.95 ppm (H-4 **G**). Thus, the  $\alpha$ -GalA **B** residue was linked at O-4 of  $\beta$ -GlcN **G** of the lipid A backbone by a phosphodiester bond. To summarize, we found that *T. hydrothermalis* LOS has



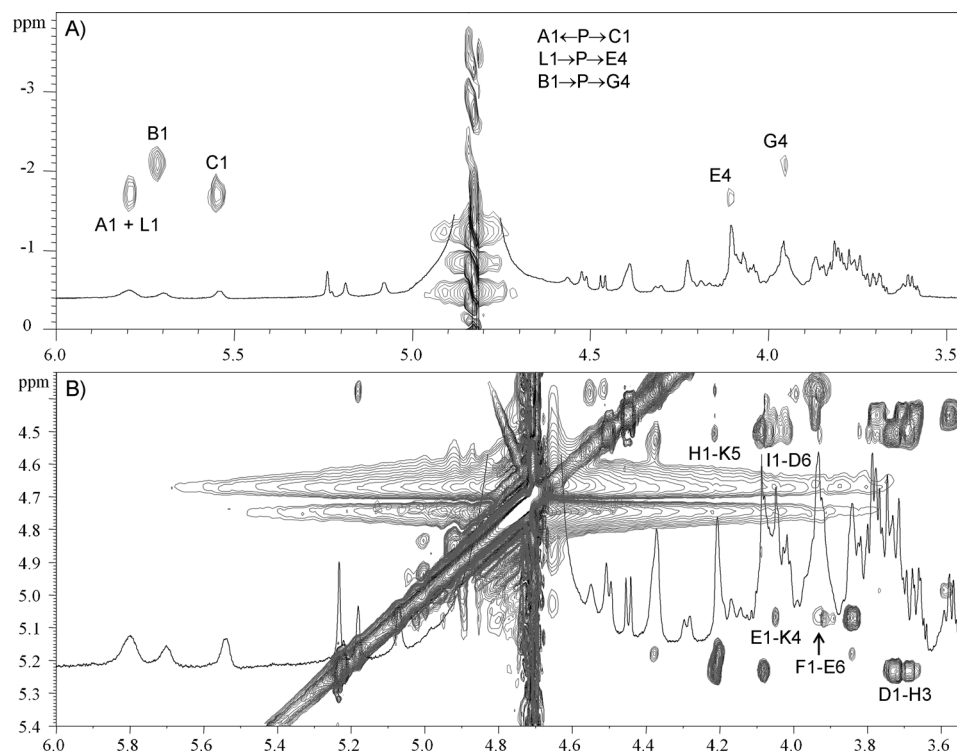


**Figure 4.** A) Section of  $^1\text{H}$  NMR and  $^1\text{H}/^{31}\text{P}$  HSQC spectra of the O-deacylated LOS from *T. hydrothermalis*. The assignment of the phosphate resonances and their correlation to their respective protons is shown. The three phosphodiester correlations are indicated center top. Anomeric signals of spin system as in Table 1. B) Section of the TOCSY (black) and NOESY (gray) spectra of the O-deacylated LOS from *T. hydrothermalis*. Spin system labels are as in Table 1. Relevant inter-residue NOE crosspeaks are shown.

a unique lipid A carbohydrate backbone characterized by the presence of the disaccharide  $[\text{P} \rightarrow 4\text{-}\beta\text{-D-GlcpN}(1 \rightarrow 6)\text{-}\alpha\text{-D-GlcpN1} \rightarrow \text{P}]$  with a galacturonic acid on each phosphate group. The location and distribution of fatty acids on lipid A remained to be ascertained.

We also performed NMR experiments on the fully deacylated lipo-oligosaccharide molecule. After a mild hydrazinolysis, complete deacylation was achieved by strong alkaline hydrolysis.<sup>[29]</sup> As expected, the harsh alkaline approach hydrolyzed all phosphodiester bonds in the molecule, and the remaining reducing oligosaccharide underwent epimerization/degradation. Full NMR characterization was impaired because of the great heterogeneity of the product. However, the  $^1\text{H}$  NMR spectrum of the fully deacylated oligosaccharide showed the ex-

pected sugar spin systems, as detected in the previous product (Figure 5).

The complete carbohydrate backbone of *T. hydrothermalis* LOS is also shown in Scheme 1.

### Structural analyses of lipid A and the core oligosaccharide by MALDI mass spectrometry

In order to reveal the fatty acid location and distribution on the lipid A moiety and obtain full confirmation on the oligosaccharide backbone, we undertook different MS experiments. An aliquot of intact LOS was analyzed by MALDI MS. The spectrum relative to the intact LOS (Figure 6A) showed, at the lower mass range, three ion peaks related to the lipid A moiety; these arose from typical fragmentation between the lipid A portion and the Kdo-containing oligosaccharide domain.<sup>[30,31]</sup> In particular, the main ion peak at  $m/z$  1925.3 (Figure 6A) was identified as a hexa-acylated bis-phosphory-

lated lipid A, with galacturonic acid residues on both phosphate groups (see  $^{31}\text{P}$  NMR above). For fatty acid number and composition, the ion peak at  $m/z$  1925.3 was characterized by the presence of two 11:0(3-OH) in ester linkage and two 11:0(3-OH) in amide linkage as primary fatty acids and two 11:0 as secondary fatty acids, in agreement with results from the fatty acid compositional analysis. The other two minor ion peaks (related to the lipid A species) were lacking one ( $m/z$  1749.4) or two ( $m/z$  1572.7) galacturonic acid residues (Figure 6A). Also detectable in this spectrum was the single ion peak related to the core oligosaccharide moiety at  $m/z$  1288.3 relative to a heptasaccharide carrying a galacturonic acid linked by a phosphodiester bridge, in agreement with the NMR analysis. At higher molecular masses (2900–3220 Da),

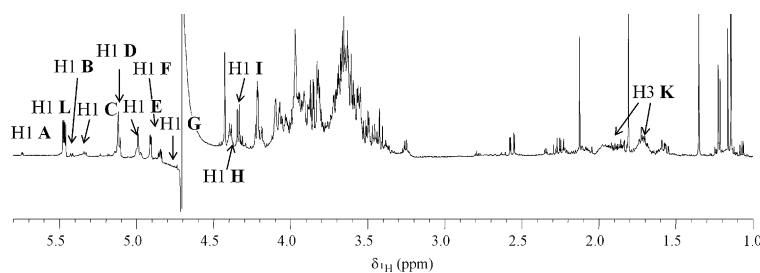
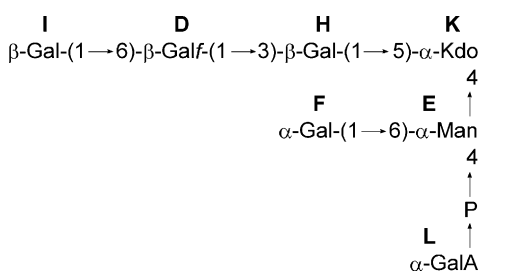


**Figure 5.**  $^1\text{H}$  NMR spectrum of fully deacylated product. The main anomeric resonances are shown.

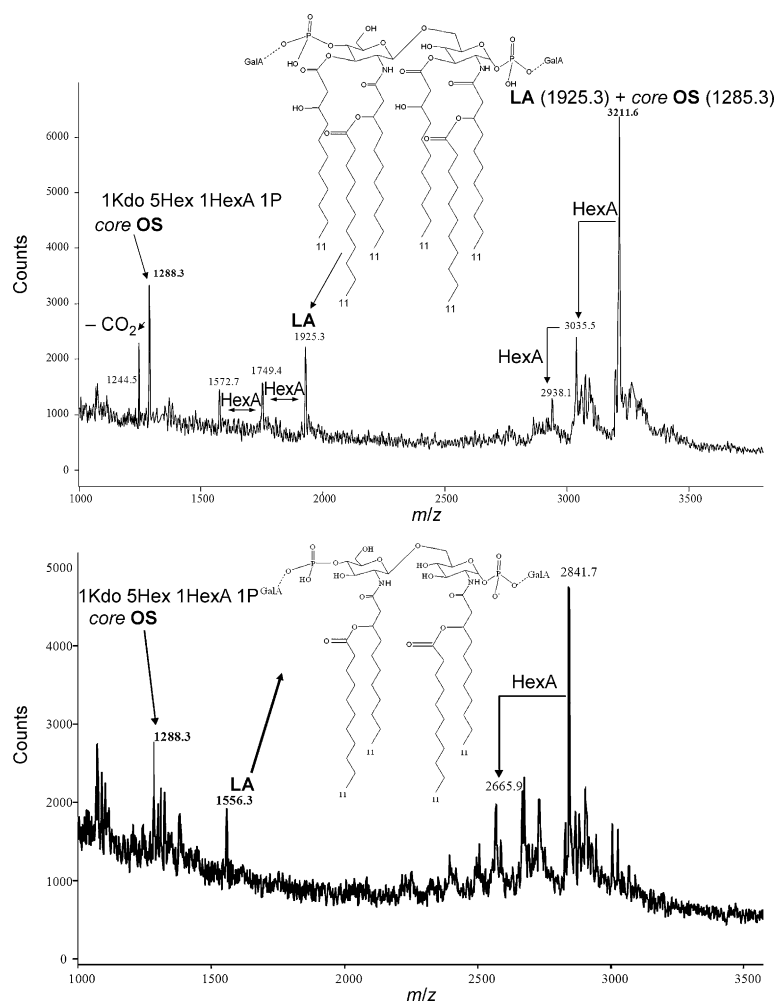


**Figure 6.** A) Negative-ion MALDI TOF spectrum of intact LOS of *T. hydrothermalis* recorded in linear mode. The Kdo-containing oligosaccharide can be easily recognized by a twin peak (44 Da less due to CO<sub>2</sub> loss from Kdo). The main lipid A species structure is sketched in the spectrum. B) Negative-ion MALDI TOF spectrum of *T. hydrothermalis* LOS after treatment with NH<sub>4</sub>OH. Lipid A structure without primary fatty acids in ester linkage is shown. Assignment of the main ion peaks is indicated.

three ion peaks were detected, corresponding to LOS species, given by the combination of core oligosaccharide and lipid A moieties (Figure 6A). The main signal ( $m/z$  3211.6) matched a LOS characterized by hexa-acylated bis-phosphorylated lipid A carrying two galacturonic acids and covalently linked to a phosphorylated hepta-saccharide core moiety. The two minor peaks ( $m/z$  3035.5 and 2938.1) were relative to LOS species, without one or two galacturonic acid residues, respectively (Figure 6A).

For the nature and the positions of the secondary acyl chains on lipid A, we analyzed the MS spectra of the complete LOS after treatment with NH<sub>4</sub>OH (Figure 6B) as described by Silipo et al.<sup>[32]</sup> This method allows selective hydrolyzation of the acyloxyacyl ester-linked fatty acids while leaving acyloxyacyl amide unaffected. The resulting MS spectrum contained, beside the expected core OS ion peak at  $m/z$  1288.3, a lipid A ion peak ( $m/z$  1556.3) attributable to a tetra-acylated species bearing two acyloxyacyl amide groups (Figure 6B). Thus, on

the basis of MS and chemical analyses, the lipid A species from *T. hydrothermalis* is shown in Figure 6A.

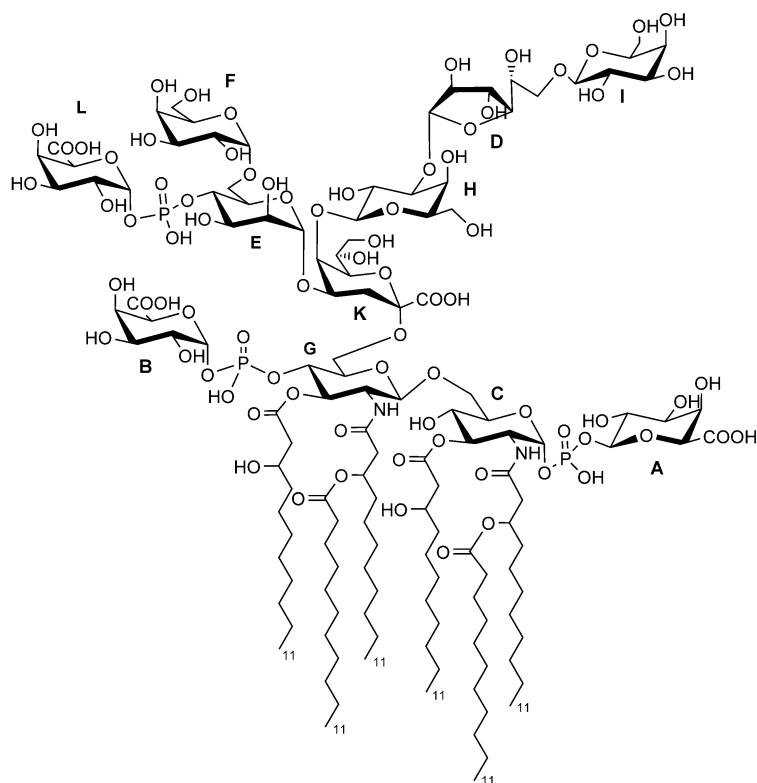
By combining the NMR data obtained for the oligosaccharide moiety with the MS data obtained for intact LOS we were able to define the complete structure of LOS from *T. hydrothermalis* (Scheme 2).

## Conclusion

The genus *Thermomonas*, established by Busse et al.,<sup>[33]</sup> comprises four Gram-negative species: *T. haemolytica*,<sup>[33]</sup> *Thermomonas brevis*,<sup>[34]</sup> *Thermomonas fusca*,<sup>[34]</sup> and *T. hydrothermalis*,<sup>[7]</sup> all of which are able to grow at temperatures as high as 50 °C. *T. hydrothermalis* was isolated from a natural thermal environment, the hot spring at São Gemil in Portugal.<sup>[7]</sup> Evolutionary bacterial adaptation to extreme temperatures implies structural variations in the outer and inner membranes of bacterial cells. As lipopolysaccharides are the main components of the outer leaflet of the external membrane of Gram-negative bacteria, it is reasonable to assume that some structural changes should also characterize LPSs isolated from thermophiles such as *T. hydrothermalis*. Consequently, elucidation

of the full chemical structure of LPSs is a crucial to dissect the molecular mechanisms underlying their essential role in the adaptation to high temperature. Furthermore, as stated above, there is intense research into the molecular aspects of TLR4 receptor activation by LPS and signaling downstream, by using LPS lipid A analogues of synthetic or natural origin.<sup>[35]</sup> In this context, we determined the complete structure of *T. hydrothermalis* LOS and established its bioactivity on innate immune system cells. Structural elucidation of LOS was achieved by a multi-techniques approach encompassing compositional analysis, NMR spectroscopy, and MALDI MS. The lipid A moiety structure was examined by MS analysis on intact LOS, and all results were corroborated by fatty acid analysis and by further MALDI MS experiments performed on partially deacylated lipopoligosaccharide. Elucidation of the core oligosaccharide skeleton was achieved by a combination of NMR experiments on O-deacylated and fully deacylated LOS, and by MALDI MS experiments on intact LOS and on its deacylated forms.





**Scheme 2.** Complete structure of *T. hydrothermalis* LOS. Monosaccharides are labeled as in Table 1.

*T. hydrothermalis* LOS is characterized by a unique structure (Scheme 2), which is composed of a hexa-saccharide skeleton in which the phosphorylated mannose residue (Scheme 2) carries an additional  $\alpha$ -galacturonic acid linked by phosphodiester linkage. Even though galactofuranose residues are biosynthesized by plants and microbes, they are very rarely found as an LPS component.<sup>[36]</sup> To the best of our knowledge, this is the first time that a galactofuranose residue has been found in the core region of a bacterial lipopolysaccharide. Furthermore, lipid A turned out to have a unique structure: two GalA residues linked by a phosphodiester bond to the archetypal backbone,  $\alpha$ -D-GalpA1  $\rightarrow$  P  $\rightarrow$  4- $\beta$ -D-GlcpN-(1 $\rightarrow$ 6)- $\alpha$ -D-GlcpN1  $\rightarrow$  P  $\leftarrow$  1- $\alpha$ -D-GalpA. It was also acylated by two C11:0(3-OH) in ester linkage and two 11:0(3-OH) in amide linkage as primary fatty acids and two 11:0 as secondary fatty acids. Thus, the overall structure of *T. hydrothermalis* LOS was shown to be highly negatively charged (at physiological pH), as it has three phosphate groups and four sugar residues bearing carboxyl groups (the Kdo and the three galacturonic acid residues). This peculiarity confers on the entire macromolecule the ability to interact with divalent cations normally present on the surface of the outer membrane. These interactions between LOS-negative charges and cations play a pivotal role in the rigidity and to the tightness of the outer membrane, resulting in bacterial high resistance to external stresses.<sup>[10]</sup> These findings might explain the *T. hydrothermalis* capability to survive in a hot spring at the temperature of 50°C.

LPS is involved in human innate immune system elicitation: hexa-acylated bis-phosphorylated lipid A from *E. coli* has a high bioactivity when binding to the TLR4/MD2 binary complex and thus triggering downstream responses. Despite a common overall molecular architecture, LPSs of different bacterial origins display a versatile array of subtle chemical modifications to fine-tune the innate immunity response. In addition, TLR4 recognizes a broad variety of substances from viruses, fungi, and mycoplasma. LPS analogues that block TLR4 activation (antagonists) are target compounds for developing drugs against acute sepsis and septic shock arising from excessive and deregulated TLR4 activation and signaling. For these reasons, we investigated the immunostimulatory activity of *T. hydrothermalis* LOS; it showed lower ability to engage the TLR4/MD-2/CD14 pathway than hexa-acylated LPS of *E. coli*. Consistent with data of TLR4 activation, in BMDMs *T. hydrothermalis* LOS elicited a low amount of inflammatory cytokine (TNF- $\alpha$  and KC), thus confirming the low biological activity of this molecule. This is an interesting result as *T. hydrothermalis* lipid A is hexa-acylated like *E. coli* lipid A, which is considered, as mentioned above, the archetypal agonist of the TLR4 complex.<sup>[37]</sup> However, several differences are responsible for the low immunopotential of *T. hydrothermalis* LOS: 1) the presence in *T. hydrothermalis* lipid A of acyl chains shorter than those of *E. coli* (11 carbon atoms vs. 14 and 12 carbon atoms); 2) the “symmetric” distribution of fatty acids of *T. hydrother-*

*malis* lipid A which is, different from *E. coli* lipid A (decorated by three acyl residues on each glucosamine molecule), and 3) galacturonic acid on both phosphate groups. Interestingly, *T. hydrothermalis* lipid A also displayed antagonistic activity versus the hexa-acylated *E. coli* LPS at low doses; this property has been extensively reported for tetra-acylated lipid A, such as Eritoran and Lipid IV<sub>A</sub>.<sup>[38,39]</sup> Several models support the activity of these molecules: competing for/disturbing the binding of the agonist LPS and preventing TLR4 dimerization.<sup>[40]</sup> Nevertheless, as the structures of the antagonistic models are totally different from that of *T. hydrothermalis* lipid A, it is hard to appreciate the mechanism that allows *T. hydrothermalis* lipid A to successfully compete with *E. coli* LPS in TLR4 binding. This supports the notion that the structures and activities of the molecular complexes (especially the intermediate forms) upon LPS binding to TLR4/MD-2 are not fully understood.

## Experimental Section

**Growth of *T. hydrothermalis* cells for LOS extraction:** Cultures of *T. hydrothermalis* SGM-6<sup>T</sup> (isolated from the hot spring at São Gemil, Portugal) used for LOS analysis were grown in 1 L Erlenmeyer flasks containing of *Thermus* medium<sup>[41]</sup> (300 mL) at 50 °C in a reciprocal water bath shaker until the late exponential phase of growth.<sup>[7]</sup> Cells were recovered and washed twice with Tris-HCl (10 mM, pH 7.5), followed by centrifugation (3000*g*, 30 min, 4 °C) and then freeze dried.

**Extraction, purification, and SDS-PAGE analysis of LOS:** Dried cells were extracted by the phenol/chloroform/light petroleum extraction protocol.<sup>[22]</sup> The extracted sample was subjected to enzymatic hydrolysis by using RNase, DNase (5 h, 37 °C) and proteases (16 h, 56 °C) in a digestion buffer (100 mM Tris, 50 mM NaCl, 10 mM MgCl<sub>2</sub>, buffer at pH 7.5 with 1 M HCl) to remove cell contaminants. Further on, dialysis and Sephacryl HR-300 chromatography were executed on the digested sample. Then it was analyzed by 13.5% SDS-PAGE to detect LPS and/or LOS by staining with silver nitrate.<sup>[23]</sup>

**Preparation of O-deacylated and fully deacylated LOS:** LOS (30 mg) was treated with anhydrous hydrazine (2 mL), stirred at 37 °C for 90 min, cooled, poured into ice-cold acetone (20 mL), and allowed to precipitate. The precipitate was centrifuged (3000 g, 4 °C, 30 min), washed twice with ice-cold acetone, dried, dissolved in water, and lyophilized.<sup>[28]</sup> The O-deacylated product was analyzed by NMR and MALDI MS, then N-deacylated with KOH (4 M). Salts were removed by gel permeation chromatography with a Sephadex G-10 column (50 × 1.5 cm; Pharmacia, Piscataway, NJ) to yield the resulting oligosaccharide.<sup>[29]</sup>

**Chemical analysis:** Determination of the sugar residues by GC-MS was carried out as described elsewhere.<sup>[24–26]</sup> Monosaccharides were identified as acetylated O-methyl glycoside derivatives. After methanolysis (HCl (1.25 M in MeOH, 85 °C, 24 h) and acetylation with acetic anhydride (25 µL) in pyridine (25 µL, 85 °C, 24 h), the sample was analyzed by GC-MS. Linkage analysis<sup>[26]</sup> was carried out by methylation of the complete saccharide portion as described previously.<sup>[26]</sup> the sample was methylated with iodomethane (300 µL, ice bath, 2 h), hydrolyzed with trifluoroacetic acid (2 M, 100 °C, 2 h), carbonyl-reduced with NaBD<sub>4</sub> (5 mg in 1 mL 50% MeOH, 4 °C, 16 h), acetylated with acetic anhydride (25 µL) and pyridine (25 µL, 85 °C, 24 h), and analyzed by GC-MS. In all analyses, GC-MS was performed with the following temperature program: 150 °C (5 min), 150 → 300 °C (5 °C min<sup>-1</sup>), 300 °C (20 min) with C11:0(3-OH) elution at 7 min or C11:0 at 4 min.<sup>[25]</sup>

**HEK 293 hTLR4/CD14/MD2 cell culture, transfection and stimulation:** Stably transfected cell lines HEK 293 hTLR4/MD-2/CD14, HEK 293 TLR2 and HEK 293 hTLR4 (InvivoGen, San Diego, CA) were cultured in DMEM with FBS (10%) supplemented with Blasticidin (10 mg mL<sup>-1</sup>; InvivoGen) and HygroGold (50 mg mL<sup>-1</sup>; InvivoGen). For NF-κB studies, cells were seeded into 96-well plates (2 × 10<sup>5</sup> cells per well) and transfected overnight with firefly luciferase reporter constructs, pGL3.ELAM.tk and *Renilla* luciferase reporter plasmid, pRLTK by using JetPEI transfection reagent.<sup>[27]</sup> HEK 293 hTLR4/MD-2/CD14 cells were exposed to different concentrations of *T. hydrothermalis* LOS or *E. coli* LPS (LPS-EB ultrapure, InvivoGen) at different concentrations (1, 10, or 100 ng mL<sup>-1</sup>) and incubated for 4 h. For the competition assay, cells were primed with *T. hydrothermalis* LOS (1, 10, or 100 ng mL<sup>-1</sup>) for 1 h and then incubated with LPS-EB ultrapure (10 ng mL<sup>-1</sup>) for 4 h. To assess the absence of contamination in LPS preparations, HEK 293 hTLR2 cells were stimulated (as described by Nigro et al.)<sup>[27]</sup> with *T. hydrothermalis* LOS or *E. coli* LPS. Pam3CSK4 (InvivoGen) was used with HEK293 hTLR2, and NF-κB-dependent luciferase activity was measured by using the Dual-Luciferase Reporter Assay System (Promega). Cell supernatants were recovered, and IL-8 was measured by using a human CXCL8/IL-8 DuoSet plate assay (R&D System, Minneapolis, MN).

**BMDMs culture and stimulation assays:** Bone marrow-derived macrophages (BMDMs) were derived from bone marrow cells collected from five-week old wild-type C57BL/6 mice (Charles River

Laboratories).<sup>[42]</sup> Animal studies were conducted according to protocols approved by the University of Rome La Sapienza and adhered strictly to the Italian Ministry of Health guidelines for the use and care of experimental animals. All efforts were made to minimize the number of animals used and their suffering. For stimulation assays, BMDMs were seeded into 24-well plates (5 × 10<sup>5</sup> cells per well) and were exposed to different concentrations of *T. hydrothermalis* LOS or *E. coli* LPS (1, 10, or 100 ng mL<sup>-1</sup>) for 18 h. Cell supernatants were recovered, and cytokine (TNF-α and KC) levels in cell culture supernatants were measured by ELISA with the DuoSet (R&D System), by following manufacturer's suggestions.

**NMR spectroscopy:** 1D and 2D <sup>1</sup>H NMR spectra were recorded in D<sub>2</sub>O at 300 K at pD 7 with a Bruker 600 DRX spectrometer equipped with a cryo-probe. The spectra were calibrated with internal acetone (δ<sub>H</sub> = 2.225 ppm; δ<sub>C</sub> = 31.45 ppm). <sup>31</sup>P NMR experiments were carried out with a Bruker DRX-400 spectrometer with phosphoric acid (85%) as the external reference (δ = 0.00 ppm). TOCSY experiments were performed with spinlock times of 100 ms with data sets of 4096 × 256 points (t<sub>1</sub> × t<sub>2</sub>). ROESY and NOESY experiments used 4096 × 256 points (t<sub>1</sub> × t<sub>2</sub>) with mixing times between 100 and 400 ms and 16 scans. Phase-sensitive DQF-COSY experiments used 4096 × 512 points. The data matrix in all the homonuclear experiments was zero-filled in both dimensions to give a matrix of 4 K × 2 K points and was resolution-enhanced in both dimensions by a cosine bell function before Fourier transformation. Coupling constants were determined by 2D phase-sensitive DQF-COSY.<sup>[43,44]</sup> HSQC and HMBC experiments were executed in <sup>1</sup>H-detection mode by single-quantum coherence with proton decoupling in the <sup>13</sup>C domain and 2048 × 256 points. Experiments were carried out in the phase-sensitive mode.<sup>[45]</sup> A 60 ms delay was used for the evolution of long-range correlations in the HMBC experiment. The data matrix in all the heteronuclear experiments was extended to 2048 × 1024 points by using forward linear prediction extrapolation.

**MALDI TOF mass spectrometry:** MALDI-TOF mass spectra of intact LOS were recorded in linear mode and negative ion polarity on a Voyager STR system (PerSeptive, Framingham, MA) equipped with delayed extraction technology. Ions formed by a pulsed UV laser beam (nitrogen laser, λ = 337 nm) were accelerated by 24 kV. R-type LPS preparation was performed as previously reported.<sup>[30,31]</sup>

## Acknowledgements

A.M., A.S., M.L.B. acknowledge COST Action BM1003 "Microbial Cell Surface Determinants of Virulence as Targets for New Therapeutics in Cystic Fibrosis". This work was partially supported by the Italian Cystic Fibrosis Foundation, Project FFC#12/2012, adopted by Delegazione FFC Novara, Latina, Imola, Pesaro, and by Associazione Trentina FC onlus in ricordo di Don Renato Vallozzi.

**Keywords:** extremophiles · glycolipids · lipopolysaccharides · structure elucidation · *Thermomonas* · thermophiles

[1] N. M. Mesbah, J. Wiegel, *Ann. N. Y. Acad. Sci.* **2008**, 1125, 44–57.

[2] K. O. Stetter, *FEBS Lett.* **1999**, 452, 22–25.

[3] a) M. P. Taylor, L. Van Zyl, M. Tuffin, D. Cowan in *Extremophiles: Microbiology and Biotechnology* (Ed.: R. P. Anitori), Caister Academic, Norfolk, **2012**, pp. 1–2; b) N. A. Eckardt, *Plant Cell* **2008**, 20, 1421–1422.

[4] T. D. Brock, *Ann. Rev. Ecol. Syst.* **1970**, 1, 191–220.

- [5] T. D. Brock in *Thermophiles: General, Molecular and Applied Microbiology* (Ed.: T. D. Brock), Wiley, New York, **1986**, pp. 1–16.
- [6] K. O. Stetter, *J. Chem. Technol. Biotechnol.* **1988**, *42*, 315–317.
- [7] M. P. Alves., F. A. Rainey, M. F. Nobre, M. S. da Costa, *Syst. Appl. Microbiol.* **2003**, *26*, 70–75.
- [8] A. Silipo, A. Molinaro in *Bacterial Lipopolysaccharides: Structure, Chemical Synthesis Biogenesis and Interaction with Host Cells* (Eds.: Y. A. Knirel, M. A. Valvano), Springer, Vienna, **2011**, pp. 1–20.
- [9] A. Silipo, A. Molinaro, *Subcell. Biochem.* **2010**, *53*, 69–99.
- [10] C. Alexander, E. T. Rietschel, *J. Endotoxin Res.* **2001**, *7*, 167–202.
- [11] M. Caroff, D. Karibian, *Carbohydr. Res.* **2003**, *338*, 2431–2447.
- [12] U. Zähringer, B. Lindner, E. T. Rietschel in *Endotoxin in Health and Disease* (Eds.: H. Brade, S. M. Opal, S. N. Vogel, D. C. Morrison), Marcel Dekker, New York, **1999**, pp. 93–114.
- [13] O. Holst, A. Molinaro in *Microbial Glycobiology: Structures Relevance and Applications* (Eds.: A. Moran, P. Brennan, O. Holst, M. von Itzstein), Elsevier, San Diego, **2009**, pp. 29–56.
- [14] U. Zähringer, B. Lindner, E. T. Rietschel, *Adv. Carbohydr. Chem. Biochem.* **1994**, *50*, 211–276.
- [15] Y. Nagai, S. Akashi, M. Nagafuku, M. Ogata, Y. Iwakura, S. Akira, T. Kitamura, A. Kosugi, M. Kimoto, K. Miyake, *Nat. Immunol.* **2002**, *3*, 667–672.
- [16] K. Brandenburg, U. Seydel, A. B. Schromm, H. Loppnow, M. H. J. Koch, E. T. Rietschel, *J. Endotoxin Res.* **1996**, *3*, 173–178.
- [17] U. Seydel, M. Oikawa, K. Fukase, S. Kusumoto, K. Brandenburg, *Eur. J. Biochem.* **2000**, *267*, 3032–3039.
- [18] O. Holst in *Endotoxin in Health and Disease* (Eds.: H. Brade, S. M. Opal, S. N. Vogel, D. C. Morrison), Marcel Dekker, New York, **1999**, pp. 115–154.
- [19] O. Holst, *Trends Glycosci. Glycotechnol.* **2002**, *14*, 87–103.
- [20] A. Silipo, G. Erbs, T. Shinya, J. Maxwell Dow, M. Parrilli, R. Lanzetta, N. Shibuya, M.-A. Newman, A. Molinaro, *Glycobiology* **2010**, *20*, 406–419.
- [21] J. R. Rose, W. J. Christ, J. R. Bristol, T. Kawata, D. P. Rossignol, *Infect. Immun.* **1995**, *63*, 833–839.
- [22] C. Galanos, O. Lüderitz, O. Westphal, *Eur. J. Biochem.* **1969**, *9*, 245–249.
- [23] R. Kittelberger, F. Hilbink, *J. Biochem. Biophys. Methods* **1993**, *26*, 81–86.
- [24] K. Leontein, J. Lönngren, *Methods Carbohydr. Chem.* **1978**, *62*, 359–362.
- [25] C. De Castro, M. Parrilli, O. Holst, A. Molinaro, *Methods Enzymol.* **2010**, *480*, 89–115.
- [26] I. Ciucanu, F. Kerek, *Carbohydr. Res.* **1984**, *131*, 209–217.
- [27] G. Nigro, L. L. Fazio, M. C. Martino, G. Rossi, I. Tattoli, V. Liparoti, C. De Castro, A. Molinaro, D. J. Philpott, M. L. Bernardini, *Cell. Microbiol.* **2008**, *10*, 682–695.
- [28] O. Holst, *Methods in Molecular Biology, Vol. 145: Bacterial Toxins: Methods and Protocols* (Ed: O. Holst), Humana, Totowa, **2000**, pp. 345–353.
- [29] O. Holst, S. Müller-Loennies, B. Lindner, H. Brade, *Eur. J. Biochem.* **1993**, *214*, 695–701.
- [30] B. W. Gibson, J. J. Engstrom, C. M. John, W. Hines, A. M. Falick, *J. Am. Soc. Mass Spectrom.* **1997**, *8*, 645–658.
- [31] L. Sturiale, D. Garozzo, A. Silipo, R. Lanzetta, M. Parrilli, A. Molinaro, *Rapid Commun. Mass Spectrom.* **2005**, *19*, 1829–1834.
- [32] A. Silipo, R. Lanzetta, A. Amoresano, M. Parrilli, A. Molinaro, *J. Lipid Res.* **2002**, *43*, 2188–2195.
- [33] H.-J. Busse, P. Kämpfer, E. R. B. Moore, J. Nuutinen, I. V. Tsitko, E. B. M. Denner, L. Vauterin, M. Valens, R. Rosselló-Mora, M. S. Salkinoja-Salonen, *Int. J. Syst. Evol. Microbiol.* **2002**, *52*, 473–483.
- [34] J. Mergaert, M. C. Cnockaert, J. Swings, *Int. J. Syst. Evol. Microbiol.* **2003**, *53*, 1961–1966.
- [35] A. Ialenti, P. Di Meglio, G. Grassia, P. Maffia, M. Di Rosa, R. Lanzetta, A. Molinaro, A. Silipo, W. Grant, A. Ianaro, *Eur. J. Immunol.* **2006**, *36*, 354–360.
- [36] M. R. Leone, G. Lackner, A. Silipo, R. Lanzetta, A. Molinaro, C. Hertweck, *Angew. Chem. Int. Ed.* **2010**, *49*, 7476–7480; *Angew. Chem.* **2010**, *122*, 7638–7642.
- [37] B. S. Park, D. H. Song, H. M. Kim, B.-S. Choi, H. Lee, J.-O. Lee, *Nature* **2009**, *458*, 1191–1195.
- [38] H. M. Kim, B. S. Park, J.-I. Kim, S. E. Kim, J. Lee, S. C. Oh, P. Enkhbayar, N. Matsushima, H. Lee, O. J. Yoo, J.-O. Lee, *Cell* **2007**, *130*, 906–917.
- [39] U. Ohto, K. Fukase, K. Miyake, Y. Satow, *Science* **2007**, *316*, 1632–1634.
- [40] S.-i. Saitoh, S. Akashi, T. Yamada, N. Tanimura, M. Kobayashi, K. Konno, F. Matsumoto, K. Fukase, S. Kusumoto, Y. Nagai, Y. Kusumoto, A. Kosugi, K. Miyake, *Int. Immunol.* **2004**, *16*, 961–969.
- [41] R. A. D. Williams, M. S. da Costa in *The Prokaryotes*, 2ednd ed(Eds: A. Balows, H. G. Trüper, M. Dworkin, W. Harder, K. H. Schleifer), Springer, New York, **1992**, pp. 3745–3753.
- [42] F. M. Marim, T. N. Silveira, D. S. Lima, Jr., D. S. Zamboni, *PLoS One* **2010**, *5*, e15263.
- [43] U. Piantini, O. W. Sørensen, R. R. Ernst, *J. Am. Chem. Soc.* **1982**, *104*, 6800–6801.
- [44] M. Rance, O. W. Sørensen, G. Bodenhausen, G. Wagner, R. R. Ernst, K. Wüthrich, *Biochem. Biophys. Res. Commun.* **1983**, *117*, 479–485.
- [45] D. J. States, R. A. Haberkorn, D. J. Ruben, *J. Magn. Reson.* **1982**, *48*, 286–292.

---

Received: May 16, 2014

Published online on August 29, 2014